Brain Stimulation 18 (2025) 937–947

Contents lists available at ScienceDirect

Brain Stimulation

journal homepage: www.journals.elsevier.com/brain-stimulation

Task-related changes in resting state connectivity are affected by temporal interference (TI) stimulation

Danielle Lauren Kurtin [a,b,*,1], Ketevan Alania [a,b,1], Edward Rhodes [a,b], Samuel Vincent [c], Ines R. Violante [d,**], Nir Grossman [a,b,***]

[a] Division of Brain Sciences, Imperial College London, London, UK
[b] UK Dementia Research Institute, Imperial College London, London, UK
[c] St Georges, University of London, London, UK
[d] School of Biomedical Engineering and Imaging Sciences, King's College London, London, UK

ARTICLE INFO

Keywords:
Temporal interference
Stimulation
Hippocampus
Memory
Functional connectivity
Networks
Resting state

ABSTRACT

Background: Resting-state metrics, such as brain network activity and functional connectivity (FC), are influenced by preceding cognitive tasks, such as memory formation. Brain stimulation can modulate brain network activity and FC during the resting state. However, it is unknown whether it can acutely modulate activity or FC traces of preceding cognitive tasks.

Objectives: We evaluated whether non-invasive temporal interference (TI) stimulation of the hippocampus can modulate hippocampal resting-state FC traces induced by a preceding hippocampally-dependent task.

Methods: We collected resting-state functional magnetic resonance imaging (rsfMRI) in twenty healthy participants before and after the performance of an associative memory task. Theta-band TI stimulation of the medial and anterior hippocampus, and sham stimulation were delivered during post-task resting state. We used permutation tests to assess differences in pairwise mutual information functional connectivity (miFC) between pre-task rsfMRI vs post-task sham. In edges with significantly different pre-vs post-task miFC, permutation tests assessed the effect of TI on post-task miFC.

Results: MiFC was significantly lower in several functional networks during post-task sham compared to pre-task baseline, including the hippocampal-connected and task-related Anterior Temporal (AT) and Posterior Medial (PM) networks. TI stimulation of the hippocampus during post-task resting state increased the miFC in the hippocampal AT and PM networks as well as other functional networks.

Conclusions: Non-invasive TI stimulation of the hippocampus during the resting state acutely modulated FC traces related to preceding hippocampal-dependent memory tasks.

1. Introduction

Resting state functional Magnetic Resonance Imaging (fMRI) captures the transient formation and dissipation of brain networks that support neural processes [1–3]. Resting-state metrics, such as brain network activity and functional connectivity (FC), are sensitive to changes in the psychological state of participants. This includes the performance of a task prior to resting state [4–9], with changes often involving regions engaged by the task [10,11]. For example, comparisons of resting state activity and FC before and after the performance of an encoding task show changes in regions involved in memory encoding [4,9,12,13].

Brain stimulation can modulate the activity and FC of resting-state brain networks [14–16]. However, it is not known whether brain stimulation can modulate resting state activity or FC traces of preceding tasks. We know that the effects of brain stimulation depend on the state in which it is delivered [17–19]. This has been demonstrated across different vigilance states, in task vs rest and between different cognitive

* Corresponding author. Division of Brain Sciences, Imperial College London, London, UK.
** Corresponding author. School of Biomedical Engineering and Imaging Sciences, King's College London, London, UK
*** Corresponding author. Division of Brain Sciences, Imperial College London, London, UK.
E-mail addresses: danielle.kurtin18@imperial.ac.uk (D.L. Kurtin), ines.violante@kcl.ac.uk (I.R. Violante), nir.grossman@imperial.ac.uk (N. Grossman).
[1] These authors contributed equally to this work.

https://doi.org/10.1016/j.brs.2025.04.010
Received 6 January 2025; Received in revised form 9 April 2025; Accepted 9 April 2025
Available online 23 April 2025

states [17]. Hence, a reasonable corollary is that the effects of brain stimulation during a post-task resting state may operate on resting state networks and/or traces of task-related connectivity.

Here, we aim to address this knowledge gap by testing whether stimulation of the hippocampus can modulate resting-state hippocampal FC traces due to a preceding memory task. We recently conducted a study where participants performed a hippocampal-dependent task while non-invasively receiving theta-band temporal interference (TI) stimulation of the hippocampus, and showed that stimulation modulated the task-evoked BOLD activity and FC [20]. Here, using data from the same participants, we investigate whether similar TI stimulation of the hippocampus but during resting state could modulate hippocampal FC induced by the preceding associative memory task.

In particular, we focused on hippocampal-cortical networks involved in memory functions, conceptualised as the Posterior Medial Anterior Temporal (PMAT) framework. The PMAT framework captures how the hippocampus coordinates two cortical networks, each of which are responsible for different aspects of memory encoding, maintenance, and recall [21–23]. The Anterior Temporal (AT) network is thought to determine the significance of stimuli, especially entities, whereas the Posterior Medial (PM) network supports the contextual embedding of stimuli in situation models [22]. Our earlier study showed that successful encoding during a hippocampal-dependent Face-Name task increased both the activity in the anterior hippocampus and hippocampal-AT FC [20]. TI stimulation administered to the anterior hippocampus during the encoding portion of Face-Name task decreased both the task-related increase in hippocampal BOLD activity and hippocampal-AT network FC. While our work and others [24] has demonstrated TI's capacity to modulate task-related activity, it is unclear whether TI can modulate resting state activity. Moreover, earlier studies stimulating the cortical-hippocampal network during resting state were not designed to test changes induced by memory tasks.

For example, Wang et al. showed that multi-day sessions of beta-band (20 Hz) Transcranial Magnetic Stimulation (TMS) of the left lateral parietal cortex during a resting state increased the fMRI FC in the cortical-hippocampal network and was associated with improvement in associative memory performance. [25]. A follow-up study by Warren et al. delivered TMS to a PM network region identified by a baseline rsfMRI scan for five consecutive days, before and 24 h after participants performed a memory task. After the stimulation paradigm, the cortical-hippocampal network FC was stronger during a memory task than in the resting state [26]. While both studies demonstrated that stimulating the cortical-hippocampal network can increase its FC and lead to behavioural benefits, it remains unclear whether stimulation can change traces of FC from preceding memory tasks during resting state.

Our experiment included a baseline (stimulation-free) resting-state fMRI, followed by a Face-Name associative memory task fMRI, and then post-task resting-state fMRI. We applied TI stimulation at the theta band to the medial hippocampus (TI 1:1 current ratio between anterior and posterior electrode pairs), anterior hippocampus (TI 1:3 current ratio), or sham stimulation in a counterbalanced order during the Face-Name task period and during the post-task period. The effect of TI hippocampal stimulation on the PMAT FC during the task was reported elsewhere [20]. Note that there was no difference in memory performance between conditions [20]. We first established the task-related changes in the resting-state FC by comparing the post-task sham to the baseline. We then tested whether the post-task TI hippocampal stimulation modulated the sham's task related changes in resting-state FC.

2. Methods

2.1. Participants

Twenty-two healthy participants were recruited for this study, as previously reported [20]. As in our previous study, one participant was excluded because of a technical failure with the MRI scanner. While one subject was excluded from the task fMRI study due to excessive movement in the scanner (see fMRI pre-processing for more information), this subject did not meet exclusion criteria during the resting state runs (see Appendix, Quality Assessment). A different subject was excluded from this work due to an inability to transform the Schaefer cortical atlas to subject space (Fig. A2). Therefore, twenty participants were included in this study (11 females, age range: 20–54 years old, mean age = 26.70, std = ±7.47, 19 right-handed and 1 left-handed). All subjects gave written, informed consent, held a minimum of a university degree, and reported no history of neurological or psychiatric illness. The study conforms to the Declaration of Helsinki and ethical approval was granted by the Imperial College Research Ethics Committee (ICREC).

2.2. TI stimulation

TI was delivered by generating two sinusoidal waveforms delivered through four electrodes placed on the participant's head as previously described [20] (Fig. 1A). Self-adhesive TENS electrodes, 1.5 cm^2 square shapes with rounded corners were affixed to participant's heads using conductive paste (Ten20, D.O. Weaver) and medical tape (3M Micropore medical tape). The first pair of electrodes, e_1 and e_2, were positioned anteriorly on the left and right side of the head respectively, and delivered a sinusoidal waveform with a frequency at 2000 Hz. The second pair of electrodes, e_3 and e_4, were positioned posteriorly on the left and right side and delivered a sinusoidal waveform with a frequency of 2005 Hz (Fig. 1A).

TI 1:1 stimulation delivered 2 mA current intensity (peak to baseline) through each pair of electrodes and with the intent to target the medial left hippocampus (Fig. 1Ai, i e., region with the largest amplitude modulated waveform). TI 1:3 delivered 1 mA to the anterior e_1-e_2 pair, and 3 mA to the posterior e_3-e_4 pair, and this 1:3 current ratio was designed to shift the peak of the amplitude modulated waveform to the anterior left hippocampus (Fig. 1Aii). In both TI conditions, a ramp up and down of 5 s initiated and ended the stimulation. Sham stimulation was equivalent to TI 1:1 stimulation, but the current was ramped down immediately after completing the ramp up.

2.3. Experimental setup and procedure

Thresholding of participant's comfort and perception of sensation to both conventional tACS and TI was conducted before the MRI portion of the experiment. For each electrode pair, stimulation was delivered at 0.1 mA. The amplitude was then increased in steps of 0.1 mA until sensations associated with stimulation were reported or maximum intensity for stimulation (2 mA for e_1-e_2 and 3 mA for e_3-e_4) was reached. The amplitude threshold at which the stimulation was perceived was lower for tACS than TI (mean ± standard deviation (std) amplitude for e1-e2: tACS = 0.44 ± 0.18 mA, sensations reported in 20 out of 20 participants; TI = 2.0 ± 0 mA, sensations reported in 1 out of 20 participants; mean ± std amplitude for e3-e4: tACS = 0.62 ± 0.27 mA, sensations reported in 20 out of 20 participants; TI = 2.75 ± 0.5 mA, sensations reported in 5 out of 20 participants) (Table A1). Participants reported fewer perceptual effects of stimulation during thresholding during TI (n = 4) as compared to tACS (n = 20) (Table A1). Out of the 5 participants who perceived the effects of TI stimulation during thresholding, 3 no longer reported perceptual sensations of TI in the scanner (Table A1).

Participants completed four resting state (rs) fMRI runs, each lasting 7 min 56 s (Fig. 1B). The first rsfMRI was stimulation free and conducted before participants performed a hippocampally-dependent Face-Name task (reported fully in Ref. [20]). Due to the variability in participant's response times, the exact duration of the Face-Name task varied across participants. The average duration of the task was 26.8 min (range 19.72–38.73 min). During the task, participants received counterbalanced blocks of sham, TI 1:1, and TI 1:3 stimulation (Fig. 1B). After performing the task, participants completed three additional rsfMRI

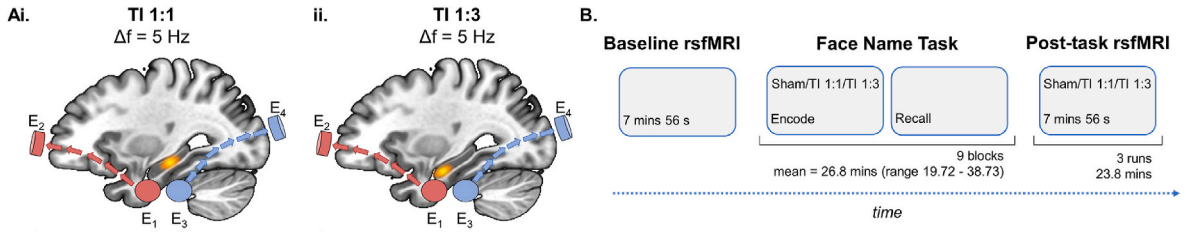

Fig. 1. (A) Diagram of electrode montage for TI 1:1 and TI 1:3 stimulation, which preferentially targets the left **(Ai)** medial and **(Aii)** anterior hippocampus, respectively. e_1 and e_3 were placed on the left hemisphere, 5 cm apart, and levelled with the plane of the nasion. e_1 was anterior to e_3 and was placed at 50 % of the subject's half circumference minus 2.5 cm and e_3 at 50 % of the subject's half circumference plus 2.5 cm. e_2 and e_4 were on the right hemisphere on a superior plane, levelled with the top of the eyebrow. e_2 was anterior to e_4 at 20 % of the subject's half circumference minus 1 cm. e_4 was positioned at 70 % of the subject's half circumference plus 1 cm. **(B)** Schematic of experimental paradigm, showing stimulation runs for pre-task baseline and post-task rsfMRI. The Face-Name task also contained blocks of sham, TI 1:1, and TI 1:3 stimulation. The order of stimulation in both task and the post-task rsfMRI were counterbalanced across participants.

runs: post-task sham, TI 1:1, and TI 1:3, the order of which was counterbalanced across participants. During rsfMRI, participants were instructed to lie still, let their minds wander, not to fall asleep, and to keep their eyes closed. After each rsfMRI run, participants were asked whether they thought they received stimulation. Effectiveness of blinding was computed using a Linear Mixed Effect Model with a binomial distribution and logit link function. The predicted value represented the accuracy in participants' rating whether they thought they did or did not receive stimulation. The fixed effect was condition (post-task sham, TI 1:1, and TI 1:3) or run number. Subject ID was used as a random effect. There was no significant effect of condition ($F(2,55) = 0.10$, $p = 0.90$) or run number ($F(2,55) = 0.10$, $p = 0.34$) on whether participants thought they received stimulation.

After the experiment, and outside of the scanner, participants completed an Adverse Events Questionnaire adapted from Ref. [27] to report the intensity and duration of the following symptoms: pain, burning, warmth/heat, itchiness, pitching, metallic taste, fatigue, effect on performance, trouble concentrating, sleepiness/fatigue, headache, mood change, or any other side effect. Participants rated symptoms on a scale from 0 to 4, to report no-severe sensations (Table A2). This questionnaire reflected sensations for the whole session and therefore we cannot infer from it whether these are related to a particular TI stimulation condition or stimulation in general.

2.4. Electric field modelling

Individual modelling of the electric (E) field for TI 1:1 and TI 1:3 stimulation was previously described [20]. In brief, the electrode placement for each participant was modelled on an anatomical, six-compartment (scalp, skull, cerebrospinal fluid, grey matter, white matter, and head cavities) model using T1 scans. The simulations were executed in Sim4Life, using the finite element method low-frequency electro-quasistatic, ohmic-current-dominated (EQSCD) solver and tissue conductivities as described in Ref. [20]. The electrodes for five participants included in this study were not visible in the MRI field of view. Since their placement could not be accounted for, they were excluded from the individual E field modelling. For the remaining 15 participants, the envelope modulation amplitude for the anterior, medial, and posterior segments of the left hippocampus was computed for the TI 1:1 and TI 1:3 conditions. The field's envelope modulation amplitude for each segment was normalised to the total hippocampal exposure. Kolmogorov-Smirnov tests showed that the distribution of E field per segment was significantly different than a normal distribution; therefore, Friedman's tests evaluated whether there was a significant main effect of segment on E field. For both TI 1:1 ($F(1,2) = 8.89$, $p = 1.00e\text{-}04$) and TI 1:3 ($F(1,2) = 30.00$, $p = 3.06e\text{-}07$), there was a significant main effect of segment on E field (Fig. A1). Post-hoc sign-rank tests indicate that in the TI 1:1 condition the E field in the medial hippocampus was significantly larger than the anterior ($p = 3.00e\text{-}3$, $z = 2.95$) or posterior hippocampus ($p = 1.00e\text{-}03$, $z = -3.23$). There was not a significant difference in E field between the anterior and posterior hippocampus during TI 1:1 ($p = 26$, $z = -1.14$). Post-hoc sign-rank tests show that for the TI 1:3 condition the E field in the anterior hippocampus was significantly larger as compared to the medial ($p = 6.55e\text{-}04$, $z = -3.41$) and posterior hippocampus ($p = 6.55e\text{-}04$, $z = -3.41$), and the E field was significantly larger in the medial vs posterior hippocampus ($p = 6.55e\text{-}04$, $z = -3.41$).

2.5. MRI acquisition

T1-weighted structural images were acquired using a magnetization-prepared rapid gradient-echo (MP-RAGE) sequence, 1 mm^3 isotropic voxel, repetition time (TR) = 2.3 s, echo time (TE) = 2.98 s, inversion time 900 ms, flip angle (FA) = 9°, field of view 256 × 256 mm, 256 × 256 matrix, 160 slices, GRAPPA acceleration factor = 2. FMRI images were obtained using a T2*-weighted gradient-echo EPI sequence, 3 mm^3 isotropic voxel, TR = 2 s, TE = 30 ms, FA = 80°, field of view 192 × 192 × 105 mm, 35 slices, GRAPPA acceleration factor = 2. A total of 230 vol (7.67 min were acquired per rsfMRI run. Field map scans were acquired to correct the echoplanar imaging (EPI) images for signal distortion (TR = 599 ms, TE = 7.65 ms, FA = 60°).

2.6. fMRI pre-processing

The fMRI Expert Analysis Tool (FEAT, Version 6.00) from the FMRIB's Software Library (FSL) [28,29] was employed for the pre-processing and analysis of the fMRI data. Pre-processing included motion correction using MCFLIRT [30], slice-time correction, removal of low-frequency drifts (high-pass filter of 0.01 Hz), smoothing with a 3D Gaussian kernel (6 mm full-width at half maximum (FWHM)). Skull stripping was performed using FSL's Brain Extraction Tool (BET) [31]. Independent Component Analysis (ICA) was conducted on each rsfMRI run using Multivariate Exploratory Linear Optimized Decomposition (MELODIC [32]). FSL's Xnoiseifier (FIX [33,34]) was trained to classify components as signal or noise using an independent cohort of twenty individuals acquired in the same scanner with the same imaging parameters. Components labelled as noise were regressed out of the timeseries, as well as 24 motion regressors and their derivatives.

In preparation for miFC analyses, the 200-region Schaefer atlas [35,36] was transformed to subject space using Advanced Normalisation Tools (ANTS [37]). The quality of transformation from the atlas to each subject's space was assessed by visual inspection. One subject's transformation yielded an atlas that consistently failed to align with their cortex, and was excluded from further analysis (Fig A.2). For the remaining 20 participants, each region in the Schaefer atlas is associated with one of 8 Yeo resting state functional networks [35,36], and assigned a corresponding label. Then, masks for the AT and PM network were overlaid on the Schaefer atlas. Regions within the AT or PM networks were reassigned a label corresponding to that network. Freesurfer's *recon_all* function [38] was employed to parcellate 14

subcortical regions (the right and left caudate, hippocampus, putamen, thalamus, pallidum, nucleus accumbens, and amygdala). Hippocampi were segmented into thirds along the longitudinal axis as follows: posterior segment: Y = −40 to −30; medial segment: Y = −29 to −19; anterior segment: Y = −18 to −4. Thus, 218 regions were used in this study. Timeseries of averaged activity from voxels belonging to each region were extracted using *fslmeants*. Timeseries were z-scored to a centre mean of 0 ± 1 std.

2.7. Mutual information FC (miFC)

MiFC was computed between every pair of regions (i.e., edge) for each subject and each condition as in our previous work [39]. MiFC is an information theoretic measure of undirected, pairwise functional connectivity that captures both nonlinear and linear relationships between regional timeseries [40–43]. As an information theoretic measure of FC, miFC quantifies connectivity as the extent to which the timeseries of one region reduces the uncertainty (i.e., entropy) in knowing the timeseries of another region. For details of how miFC was computed see Ref. [39]. In brief, miFC was computed by representing each BOLD timeseries as a continuous probability density function (using Gaussian kernel density estimation). Then, the extent to which different levels of activity co-occur between two regions' probability density functions were quantified (i.e., the joint probability), followed by the frequency that each level of activity occurs in each region independently (i.e., the marginal probability). If the joint probability of two regions' activity levels is much greater than the product of each region's marginal probability, this means knowing the activity level of one region also confers confidence about the activity level of another region, i.e., there is high mutual information between them. This approach defines connectivity using similar principles as other connectivity metrics – if regions tend to co-activate and deactivate synchronously, we infer they are similarly engaged. What sets miFC apart is its ability to capture nonlinear, non-monotonic patterns of coactivation. The brain is comprised of nonlinear, dynamical interactions [44], and the increased sensitivity of miFC to these interactions heightens its ability to capture patterns undetected by conventional correlation-based metrics of connectivity.

2.8. Quality assessment

Detailed descriptions and statistical analyses of the quality assessment of the fMRI data is available in Appendix: Quality Assessment, and Table A3. Quality assessment was performed on the fMRI data both before and after pre-processing. Before pre-processing, head motion was estimated using FSL motion outliers through Framewise Displacement (FD) and the spatial root mean square of the data after temporal differencing (DVARS) using fsl_motion_outliers [45], and the number of noise components identified by ICA AROMA for each subject. No subjects met the criterion for excessive motion (DVARS >0.5 in >20 % of their volumes), the average FD (Fig A3A) and DVARS (Fig A3B) across participants was low [45,46], and there was no significant effect of run on the number of noise components per subject (Fig A3C).

After preprocessing, Intraclass Correlation Coefficient (ICC) scores were computed in line with [47] to assess the reliability in each region's timeseries across subjects. Mean ICC scores exhibited moderate reliability across subjects, suggesting low enough between-subject variability within each region's timeseries to capture group-level effects [47] (Fig A3D). Then, the global temporal signal to noise ratio (tSNR) was extracted as a metric of the stability and quality of the signal over time (Fig A3E). We found no significant relationship between differences in tSNR between runs and the significant changes in miFC.

2.9. Graph metrics

2.9.1. Route efficiency

Route efficiency captures the efficiency of moving through a graph. Route efficiency was computed using the Brain Connectivity Toolbox (BCT) as the mean of the topological length of the shortest possible path between every pair of regions. Path length considers the miFC between nodes, where higher/lower miFC imparts a lower/higher cost of travelling between nodes.

2.9.2. Modularity

Modularity (Q) was computed with the BCT [48]. Modularity quantifies the extent to which a graph (i.e., FC matrix) matches the optimal topology. The optimum is when discrete subdivisions of nodes maximises/minimises the number of within/between-group edges, respectively.

2.9.3. Global connectivity

Global connectivity was computed as the average connectivity across all pairs of regions per subject. Global connectivity is thought to reflect the synchronization across functional networks [49,50].

2.9.4. Betweenness centrality

Betweenness centrality is a measure of a node's importance in coordinating communication within a graph. A node's betweenness centrality is computed as the proportion of all shortest paths in a network containing the node.

2.10. Null models and control analyses

Null models were used to test whether the effect of run on miFC reflected topological properties or functional differences. The null model was created by randomising each timeseries, which retains the power spectra and autocorrelation of the timeseries, but randomises temporal dependencies [51–53]. Timeseries randomisation was conducted by first filtering the signal with a second-order Butterworth filter between 0.02 and 0.1 Hz, performing a fast Fourier transform on the signal, shuffling the phase coefficients, and then taking the inverse transform to the time domain. Pairwise miFC was computed as above, and permutation tests evaluated the effect of run on pairwise miFC. This procedure was run for 1000 permutations, generating a distribution of p-values for each edge. Significance of the difference between the empirical vs null p-value for the effect of run on miFC was computed as the proportion of p-values less than the empirical p-value. We found in 99.72 % of the edges with significantly different miFC were significantly different than the null model, suggesting that the effect of run on miFC drove the differences in miFC, as opposed to inherent properties of network topology.

To evaluate the extent to which results may have been influenced by employing miFC as a connectivity metric, we also computed pairwise FC between the z-scored timeseries using Spearman's ρ, a classical, correlation-based measure of connectivity. Spearman's ρ was chosen over Pearson's correlations given that Spearman's correlations are less susceptible to the influence of outliers [54,55]. Results presented in the main text were broadly replicated in correlation-based control analyses. Detailed comparisons are reported in the Appendix: Control analyses: comparing FC metrics, and Table A4.

We ran a control analysis to inform the extent to which changes in miFC were due either to TI stimulation or the influence of performing a task on resting state miFC. This control analysis was performed by first computing the ΔSham_miFC (baseline miFC - post-task sham mIFC), ΔTI1:1_miFC (post-task sham miFC - post-task TI 1:1 miFC), and ΔTI1:3_miFC (post-task sham miFC - post-task TI 1:3 miFC). We then ran permutation tests comparing ΔSham_miFC vs ΔTI1:3_miFC, and ΔSham_miFC vs ΔTI1:1_miFC among edges that showed a significant difference in miFC between baseline to post-task sham. A positive t-stat

indicated the change from baseline to post-task sham (i.e., ΔSham_miFC) was greater than the change from post-task sham due to TI 1:1 or TI 1:3 (i.e., ΔTImiFC). Results are presented in Appendix: Control analyses: comparing changes due to task or TI stimulation, and Table A5.

A control analysis evaluated whether the counterbalanced presentation of post-task runs (i.e., post-task sham, TI 1:1, and TI 1:3) sufficiently controlled for the potential effect of order on miFC. First, a Kolgov-Smirnov tested the null hypotheses that the distribution of miFC across participants was normal. If the null hypothesis was rejected, an inverse rank transformation normalised the distribution of miFC across participants. Then, a linear mixed effects model with a normal distribution and Gaussian link function evaluated the main effect of run and order as on miFC, and included subject as a random effect. All p-values were FDR-adjusted to correct for multiple comparisons. There were no edges with a significant effect of run that also showed a significant effect of order (Table A6).

2.11. Statistical analyses

All analyses were run in MATLAB2023a. Permutation tests assessed whether there was a significant difference in pairwise miFC, correlation-based FC, and all whole-brain graph metrics between baseline vs post-task sham, post-task sham vs TI 1:1, and post-task sham vs TI 1:3 conditions. Permutation tests evaluated whether there was a significant difference in the betweeness centrality in each hippocampal segment and region in the AT and PM networks between post-task sham to TI 1:1 and TI 1:3 conditions. For all analyses using permutation tests, the risk of family wise Type 1 errors due to multiple comparisons was controlled using max-T/min-P method [56]. Spearman's correlations assessed relationships between E field and miFC.

3. Results

3.1. Associative memory task attenuated functional connectivity in succeeding resting-state

We first examined whether miFC differed between baseline and post-task sham condition, reasoning that changes in regions engaged by the Face-Name task (e.g., the hippocampus, PM, or AT networks) would provide evidence that task performance influences resting-state FC. We first describe whether miFC significantly increased or decreased after the task, and which resting state functional networks show the greatest number of edges with significantly different miFC. This contextualises the extent to which the hippocampus and its segments contributed to the number of significantly affected edges, and whether significant changes in hippocampal miFC are to AT or PM network regions. Finally, we assess the extent to which significant changes in miFC include AT or PM network regions.

We found significant differences in the miFC of 1767 edges in the post-task sham compared to pre-task baseline (Table A7). Most edges (1750, 99 %) showed significantly decreased miFC, and were broadly distributed (Fig. 2Ai). The Default Mode Network (DMN), Salience/Ventral Attention Network (SN), and Control Network contributed the most regions to edges with significantly decreased miFC (15 % of edges for each network (Fig. 2Bi)).

The networks with the second-greatest contribution include the subcortical and Somatomotor networks (12 % of edges for each network (Fig. 2Bi)). Out of the subcortical regions with significantly lower miFC from pre-to post-task sham, the left and right hippocampus (inclusive of all segments) contributed to 86 and 218 edges (17 % and 44 % of subcortical edges, respectively), which is greater than all other regions with significantly lower miFC from pre-to post-task sham.

Out of the hippocampal segments, the anterior hippocampus showed the greatest changes in miFC. The left and right anterior hippocampus contributed to 22 % (66 edges) and 33 % (100 edges) of hippocampal regions with significantly affected miFC, respectively (Fig. 3). Some edges with significant differences in miFC from the left and right anterior hippocampus included regions in the PM (8 and 13 edges, respectively) and AT (1 and 5, respectively) networks (Fig. 2C). After the anterior hippocampus, the medial hippocampus contributed the second-greatest number of hippocampal edges with significantly different miFC. The left and right medial hippocampus contributed to 1 % (2 edges) and 28 % (84 edges) of hippocampal regions with significantly affected miFC, respectively. These edges included regions in the PM (7 edges from the right medial hippocampus) and AT (4 edges from the right medial hippocampus) networks (Fig. 2C; Fig. 3). The left and right posterior hippocampus had 18 edges and 34 edges with significant differences in miFC between pre- and post-task sham (6 % and 11 % of hippocampal regions with significantly affected miFC, respectively). These edges included PM (3 edges from the right posterior hippocampus) and AT regions (1 and 2 edges from the left and right posterior hippocampus, respectively) (Fig. 2C; Fig. 3).

Edges containing a PM or AT network region contributed to 11 % and 6 % of significantly different edges between pre- and post-task sham, respectively (Fig. 2Bi). While the PM and AT networks did not contribute the most significant number of regions to edges with significantly different miFC, 90 % of regions in the PM and 81 % of regions in the AT network were included in edges with significantly different miFC from baseline pre-to post-task sham.

Taken together, performing a hippocampally-dependent task generally decreased resting state miFC. These decreases included edges between the hippocampus and the PM and AT networks.

3.2. TI stimulation of the medial hippocampus during post-task resting-state modulated the task-related functional connectivity

Out of the 1767 edges with significantly different miFC between pre- and post-task sham, we identified 87 edges (5 %) with significantly different miFC between post-task sham and TI 1:1 targeting the medial hippocampus (Fig. 2Aii) (Table A7).

Most edges with significantly different miFC showed TI 1:1 stimulation increased miFC compared to post-task sham (86 edges, 99 %). The DMN showed the greatest contribution of regions with significantly higher miFC (19 % of edges) (Fig. 2Bii). After the DMN, the Control (15 % of edges) and subcortical networks (14 % of edges) contributed the most regions to edges with significantly higher miFC due to TI 1:1 (Fig. 2Bii). The left and right hippocampus were the subcortical regions that contributed to the greatest number of significantly different edges between post-task sham and TI 1:1 (4 and 3 edges, respectively).

Out of the hippocampal segments, the left and right anterior hippocampus showed the greatest number of changes in miFC (4 and 1 edges, respectively), followed by the right medial (1 edge) and right posterior hippocampal segments (1 edge) (Fig. 3). The edge with significantly different miFC from the posterior hippocampal segment was to a PM network region, the right orbitofrontal cortex.

The AT network doubled the proportion of regions contributing to significantly affected edges, from 6 % when comparing baseline pre-task vs post-task sham, to 12 % when comparing TI 1:1 to post-task sham (Fig. 2Bii). The PM network decreased the proportion of regions contributing to edges with significantly affected miFC, from 11 % in baseline to post-task sham comparisons to 9 % in post-task sham to TI 1:1 (Fig. 2Bii).

3.3. TI stimulation of the anterior hippocampus during post-task resting-state also modulated the task-related resting-state functional connectivity

Out of the 1767 edges with significantly different miFC between baseline pre- and post-task sham, we identified 62 edges (4 %) with significantly different miFC between post-task sham and TI 1:3 targeting the anterior hippocampus (Fig. 2Aiii) (Table A7).

Most edges with significantly different miFC between post-task sham

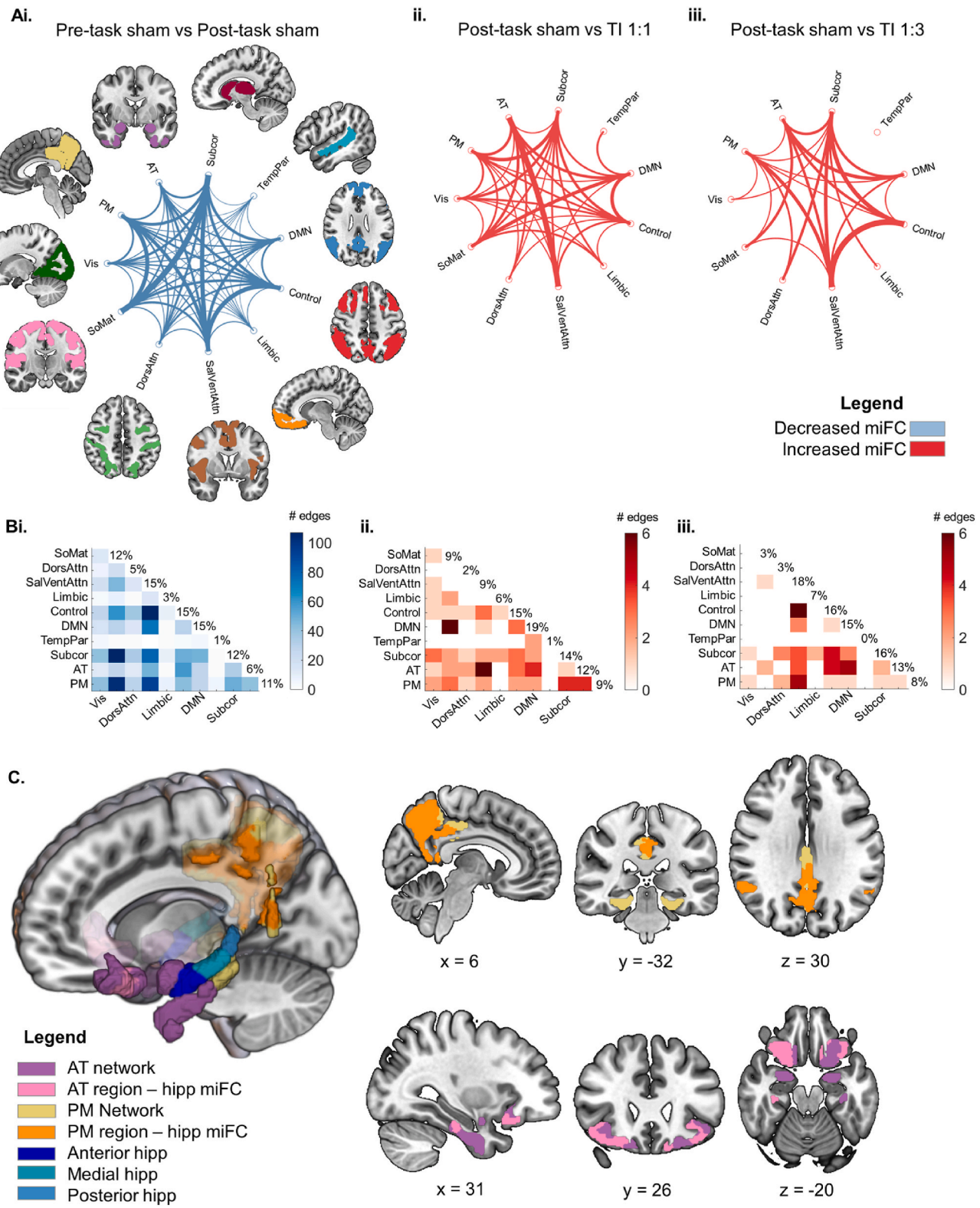

Fig. 2. There were significant decreases in miFC during **(Ai)** post-task sham vs baseline, some of which were significantly increased from post-task sham to **(Aii)** TI 1:1 or **(Aiii)** TI 1:3 stimulation. All regions are grouped into a functional network, and differences in miFC between regions in different functional networks are shown with lines between the networks. The thickness of the line scales with the number of regions showing significant differences in miFC. The colour indicates whether miFC increased (red) or decreased (blue). **(B)** The number of edges with significantly different between-network miFC in **(Bi)** baseline vs post-task sham, **(Bii-iii)** and post-task sham vs TI 1:1 and TI 1:3, respectively. The proportion of regions contributed to all significantly affected edges in each network is displayed as a percent on the right side of the matrix. **(C)** Between baseline to post-task sham miFC decreased between the hippocampus and regions in the PM (yellow) and AT networks (pink). Regions in the PM and AT network with significantly lower miFC to the hippocampus are shown in orange and pink, respectively. Hipp = hippocampus; SoMat = somatomotor; SalVentAttn = Salience/Ventral attention; DorsAttn = dorsal attention; Vis = visual; SubCor = subcortical.

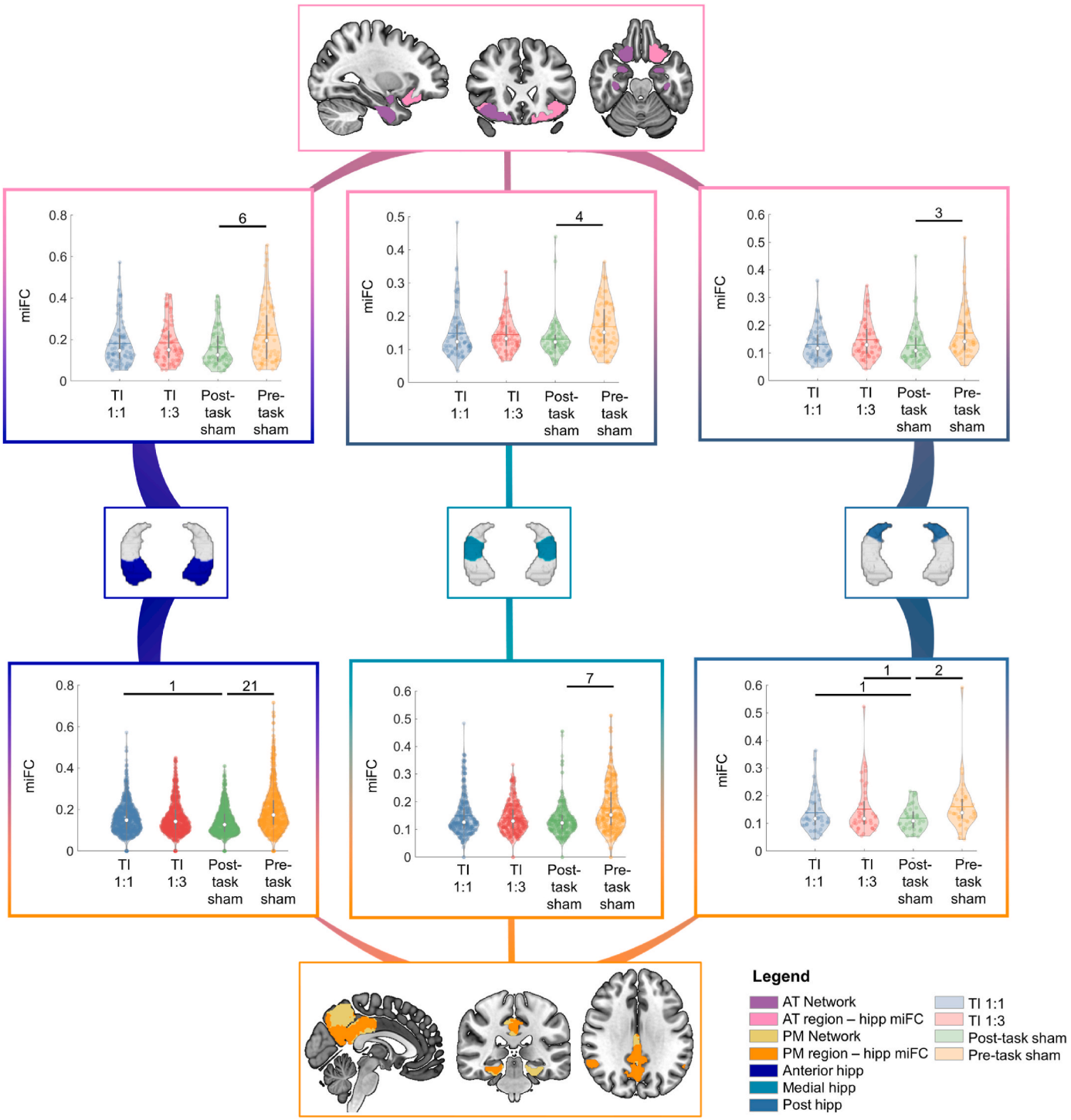

Fig. 3. Violin plots showing the effect of run on miFC between hippocampal segments and regions in the AT and PM network. Violin plots show the aggregate results for the left and right hippocampal segments. The AT or PM regions (pink and yellow, respectively) that are included are those that showed a significant decrease in miFC from pre-task baseline (orange violins) to post-task (green violins) sham. The number of AT or PM regions showing significant decreases from baseline to post-task sham is displayed over a horizontal line between the baseline and post-task sham violins. The number of AT or PM regions with significant decreases from post-task sham to TI 1:1 (blue violins) or TI 1:3 (red violins) is displayed over a horizontal line between the two runs. The top and bottom edges of the boxes in the violin plots represent the 25th and 75th percentiles, with the mean shown as the white dot and the median by the horizontal line. Extension of the whiskers indicates 1.5 the interquartile range. A kernel density estimate of the data provides the edges to the violin plot. Datapoints representing each participant's miFC between the hippocampal segment and AT or PM region are shown.

and TI 1:3 showed TI 1:3 stimulation increased miFC (59 edges, 95 %). The Salience/Ventral Attention network contributed the greatest number of regions with significantly increased miFC (18 % of edges), followed by the Control and subcortical networks (16 % of edges each) (Fig. 2Biii). Out of the edges with significantly different miFC between post-task sham and TI 1:3 that included a subcortical region, 13 (57 % of edges) included a hippocampal segment. The left and right hippocampi were the subcortical regions contributing the greatest number of

significantly different edges between the post-task sham and TI 1:3 (3 and 10 edges, respectively).

Hippocampal segments with significantly higher miFC than post-task sham due to TI 1:3 stimulation included the left anterior (3 edges), right anterior (5 edges), right medial (3 edges), and right posterior (2 edges) segments (Fig. 3). The right anterior and posterior segments each contained one edge with a significant increase in miFC to a PM network region.

When comparing post-task sham to TI 1:1, the AT network increased the proportion of regions contributing to edges with significantly increased miFC from post-task sham to TI 1:3 (from 6 % to 13 % of edges) (Fig. 2Biii). Similarly, the PM also decreased in the proportion of regions contributing to edges with significantly increased miFC from post-task sham to TI 1:3 (11 %–8 % of edges) (Fig. 2Biii).

3.4. TI stimulation modulation of task-related resting-state FC was not correlated with estimated E field amplitudes

There were no significant relationships between the estimated E field generated by TI 1:1 stimulation of the left medial hippocampus and the change in miFC from post-task sham to TI 1:1 (Table A8); nor were there any significant relationships between the E field generated by TI 1:3 stimulation of the left anterior hippocampus and the change in miFC from post-task sham to TI 1:3 stimulation (Table A9).

3.5. Differences in local, but not whole-brain, graph metrics

Permutation tests showed no significant difference in route efficiency, modularity, or global connectivity between baseline pre- and post-task sham, post-task sham to TI 1:1, or post-task sham to TI 1:3 (Table A10).

We evaluated the effects of TI on betweeness centrality, a local graph theoretic measure, in each hippocampal segment and region in the AT and PM networks. There was significantly lower betweenness centrality in the left anterior hippocampus during TI 1:1 vs post-task sham, and significantly greater betweeness centrality in 2 AT regions and 1 p.m. region during TI 1:1 vs post-task sham (Table A11). During TI 1:3 stimulation betweenness centrality was significantly greater in 1 AT and 1 p.m. region, and significantly lower in 1 AT and 2 p.m. regions, as compared to post-task sham (Table A11).

4. Discussion

This study evaluated whether stimulation of the hippocampus during resting state after the performance of a hippocampal-dependent task can influence the task-related changes in resting state FC. We found that a memory task reduced resting-state miFC across the hippocampal networks and other networks and that non-invasive TI stimulation of the hippocampus attenuates some of the task-related miFC reductions. To our knowledge, this is the first demonstration that brain stimulation can modulate resting state FC influenced by preceding cognitive tasks.

Our findings that post-task resting state FC was different than pre-task resting state FC aligns with previous work [4–9]. The changes in FC due to the hippocampal-dependent task included the hippocampus and most regions in the AT and PM networks.

Out of all regions, the hippocampus showed the greatest number of changes in miFC from baseline to post-task sham. This aligns with a recent study which also showed the hippocampus had the greatest number of changes in FC in resting state runs acquired after an encoding task [12]. Moreover, in both Folvik et al. and this work, core regions of the DMN and PM network (e.g., praecuneus) showed decreased resting state FC to the hippocampus after an encoding task [12].

However, the study by Folvik and colleagues found resting state FC increased from pre-task to post-task in many cortical networks (e.g., Salience/Ventral Attention, Control, Somatomotor, etc), whereas we observed decreased post-task miFC compared to baseline. Folvik et al. suggested that, while there is not a one-to-one link between the BOLD signal and neural activity, it was likely that post-task increases in hippocampal connectivity to cortical networks reflected hippocampal replay and reactivation of task processes, as part of awake memory consolidation [12]. This would suggest that our connectivity results reflect a lack of memory consolidation in our experiment. However, since stronger between-network connectivity reflects increased coordination across the processes supported by each network, it is unclear why baseline miFC would be stronger than post-task sham miFC. While future work is necessary to disentangle this discrepancy between this work and that of Folvik et al. for the direction of the effect of task on resting state FC between the hippocampus and cortical networks, both studies observed that resting state FC is altered in regions involved in performing a memory task [12].

Our results showed that both medial hippocampus stimulation (TI 1:1) and anterior hippocampus (TI 1:3) stimulation increased resting state miFC relative to sham in the PMAT regions. Notably, the anterior hippocampus was the hippocampal segment with the greatest number of significantly affected edges out of all subcortical regions for both TI 1:1 and TI 1:3. The anterior hippocampus is more strongly connected to the AT vs the PM network [21,22]. Both TI 1:1 and TI 1:3 significantly increased miFC of regions in the AT from post-task sham; moreover, the proportion of edges in the AT that were significantly different from post-task sham to either TI run was greater than the proportion of AT edges with significantly different miFC from baseline to post-task sham. The greater proportion of miFC changes in the AT vs PM network are consistent with the selective engagement of the Face-Name task with the AT network [20]. Collectively, these results suggest that TI stimulation did not exacerbate the post-task decrease in resting state miFC; instead, TI stimulation increased miFC towards that observed in both baseline resting state miFC and Face-Name task performance. Given that regions where TI stimulation attenuated task-related reductions in resting state miFC were concentrated among hippocampal and PMAT regions involved in task performance, TI stimulation may have enhanced task-related miFC. The reinforcement of task-related miFC during resting state aligns with previous stimulation studies of PMAT regions [25,26].

The effects of TI stimulation on local, but not global, graph network metrics also suggest that the effects of TI stimulation were concentrated in task-related circuitry. We found that TI stimulation significantly changed local graph network metrics capturing the importance of the anterior hippocampus and PMAT regions. Despite these local changes, and broad decreases in post-task resting state miFC, we did not see a difference in global measures of the efficiency of brain function between runs. This accords with work that showed performance of a semantic matching task decreased rsfMRI FC among regions in the DMN and PM, but did not change global efficiency [57].

It is important to consider the extent to which the study design may have influenced the differences in miFC observed between baseline and post-task sham. While we attributed differences in miFC between baseline and post-task sham to the performance of the Face-Name task, it is also possible that changes in miFC were associated with the elapsed time between runs, or with the TI stimulation administered during the task. However, given work showing the stability of resting state FC [58–60], we believe it is more likely that differences in miFC between baseline and post-task sham are attributed to task performance rather than the effect of time.

For example, previous work found no significant difference in the stability of within-network resting state FC within- and between sessions (e.g., resting state with eyes open, eyes closed, and eyes open on a fixation cross) in attention, DMN, Somatomotor, or Visual network connectivity [59]. Another study assessing the temporal stability of resting state FC patterns split edges into the following three groups: stable, weak, positive connections; unstable, strong, positive connections; unstable negative connections [58]. There was an order of magnitude more edges in the stable-but-weakly connected group vs the other two [58].

Unstable connections were predominantly observed between regions in the Visual and Control network [58]. The significant differences in miFC between baseline and post-task sham were not concentrated between the Visual and Control network, suggesting results were not strongly influenced by variability in network connectivity over time. Within the context of these studies and other work showing the stability of resting state FC between sessions [60], we believe it is more likely that differences in miFC between baseline and post-task sham are attributed to performing the Face-Name task rather than the time it took to complete it.

While it is possible that TI stimulation administered during the task may have influenced miFC between baseline and post-task sham, it is not likely. The counterbalanced and interleaved conditions of stimulation during the task were intentionally structured to reduce the likelihood of carryover from one block to another, as well as from the task to post-task resting state. Moreover, during each block stimulation was delivered during encoding, but not recall, effectively creating a washout period where the effects of stimulation could dissipate within each block. The results presented in Ref. [20] suggest the study design effectively reduced the potential confounds introduced by cumulative stimulation and carryover. For example, significant modulation of the magnitude of the BOLD signal by TI stimulation was only apparent during TI 1:3, but not TI 1:1, conditions [20]. Moreover, the effect of TI 1:3 was limited to modulating the magnitude of the BOLD signal during the encoding-related engagement of the anterior hippocampus, with no significant TI-related changes in the magnitude of the BOLD signal during the recall portion of the block [20]. Finally, there was no effect of stimulation on task performance during the fMRI portion of the task, reducing the likelihood that changes in the BOLD signal were attributed to non-stimulation factors that improve task performance (e.g., attention or arousal) [61]. While the results presented here and in Ref. [20] favour the interpretation that changes in miFC are related to performing the Face-Name Task, the experimental design precludes definitive separation of task, time, and stimulation carryover effects for the baseline vs. post-task sham comparison.

To evaluate whether stimulation-mediated miFC reflects behaviourally relevant consolidation processes, future work should assess whether post-task TI stimulation improves long-term accuracy of Face-Name task performance. Previous work has shown that periods of wakeful rest after a memory task improve delayed recall accuracy [9,62,63]. Additionally, work has shown that enhanced task-relevant FC through PM network stimulation was positively associated with improved task performance [25,26]. It is worthwhile to investigate whether TI stimulation could enhance the consolidation of newly acquired information during resting state, given the potential benefits for people with impairments in memory (e.g., Alzheimer's Disease).

In summary, we showed resting state miFC in the hippocampal PMAT networks was reduced after the performance of an episodic memory task. TI stimulation of the hippocampus attenuated the post-task reduction in resting state miFC in the hippocampal PMAT networks. While this is in line with work showing stimulation of PMAT networks enhances memory consolidation processes, future work is needed to characterise the behavioural effects of TI stimulation.

CRediT authorship contribution statement

Danielle Lauren Kurtin: Writing – review & editing, Writing – original draft, Visualization, Software, Methodology, Formal analysis, Data curation, Conceptualization. **Ketevan Alania:** Writing – review & editing, Methodology, Investigation, Formal analysis, Data curation. **Edward Rhodes:** Writing – review & editing, Investigation. **Samuel Vincent:** Writing – review & editing, Investigation. **Ines R. Violante:** Writing – review & editing, Supervision, Software, Methodology, Investigation, Formal analysis, Data curation, Conceptualization. **Nir Grossman:** Writing – review & editing, Supervision, Methodology, Funding acquisition, Conceptualization.

Data and code availability

Data and code to reproduce the analysis and figures in this work are available at https://github.com/ISN-Group/rsfMRI-TI. The data stored in the repository consists of the extracted timeseries for each subject, from each region of interest.

Funding

D.L.K. is supported by the National Institute for Health and Care Research (NIHR) Imperial Biomedical Research Centre (BRC) Brain Sciences Pilot Grant. I.R.V. was supported by the Biotechnology and Biological Sciences Research Council (BB/S008314/1). N.G. is supported by the UK Dementia Research Institute (UK DRI), an initiative funded by the Medical Research Council, Alzheimer's Society and Alzheimer's Research UK, NIHR Imperial BRC, and the American Alzheimer's Association.

Declaration of competing interest

N.G. is an inventor of a patent on the technology, assigned to MIT. N. G. is a co-founder of TI Solutions AG, a company committed to producing hardware and software solutions to support TI research. The remaining authors declare no competing interests.

Acknowledgements

We wish to thank the staff at the Clinical Imaging Facility (CIF), where the MRI data was collected. We appreciate all study participants for their time and contribution to this work.

Appendix A. Supplementary data

Supplementary data to this article can be found online at https://doi.org/10.1016/j.brs.2025.04.010.

References

[1] Dong H-M, Margulies DS, Zuo X-N, Holmes AJ. Shifting gradients of macroscale cortical organization mark the transition from childhood to adolescence. Proc Natl Acad Sci 2021;118:e2024448118. https://doi.org/10.1073/pnas.2024448118.
[2] Shahsavarani S, Thibodeaux DN, Xu W, Kim SH, Lodgher F, Nwokeabia C, Cambareri M, Yagielski AJ, Zhao HT, Handwerker DA, Gonzalez-Castillo J, Bandettini PA, Hillman EMC. Cortex-wide neural dynamics predict behavioral states and provide a neural basis for resting-state dynamic functional connectivity. Cell Rep 2023;42. https://doi.org/10.1016/j.celrep.2023.112527.
[3] Vohryzek J, Cabral J, Vuust P, Deco G, Kringelbach ML. Understanding brain states across spacetime informed by whole-brain modelling. Philos. Trans. R. Soc. Math. Phys. Eng. Sci. 2022;380:20210247. https://doi.org/10.1098/rsta.2021.0247.
[4] Cecchetto C, Fischmeister FPhS, Reichert JL, Bagga D, Schöpf V. When to collect resting-state data: the influence of odor on post-task resting-state connectivity. Neuroimage 2019;191:361–6. https://doi.org/10.1016/j.neuroimage.2019.02.050.
[5] Grigg O, Grady CL. Task-related effects on the temporal and spatial dynamics of resting-state functional connectivity in the default network. PLoS One 2010;5:e13311. https://doi.org/10.1371/journal.pone.0013311.
[6] Lor CS, Zhang M, Karner A, Steyrl D, Sladky R, Scharnowski F, Haugg A. Pre- and post-task resting-state differs in clinical populations. NeuroImage Clin 2023;37:103345. https://doi.org/10.1016/j.nicl.2023.103345.
[7] Požar R, Kero K, Martin T, Giordani B, Kavcic V. Task aftereffect reorganization of resting state functional brain networks in healthy aging and mild cognitive impairment. Front Aging Neurosci 2023;14.
[8] Sarabi MT, Aoki R, Tsumura K, Keerativittayayut R, Jimura K, Nakahara K. Visual perceptual training reconfigures post-task resting-state functional connectivity with a feature-representation region. PLoS One 2018;13:e0196866. https://doi.org/10.1371/journal.pone.0196866.
[9] Tambini A, Ketz N, Davachi L. Enhanced brain correlations during rest are related to memory for recent experiences. Neuron 2010;65:280–90. https://doi.org/10.1016/j.neuron.2010.01.001.
[10] Liu Y, Dolan RJ, Kurth-Nelson Z, Behrens TEJ. Human replay spontaneously reorganizes experience. Cell 2019;178:640–652.e14. https://doi.org/10.1016/j.cell.2019.06.012.

[11] Tambini A, Davachi L. Awake reactivation of prior experiences consolidates memories and biases cognition. Trends Cognit Sci 2019;23:876–90. https://doi.org/10.1016/j.tics.2019.07.008.
[12] Folvik L, Sneve MH, Ness HT, Vidal-Piñeiro D, Raud L, Geier OM, Walhovd KB, Fjell AM. Sustained upregulation of widespread hippocampal-neocortical coupling following memory encoding. Cereb. Cortex N. Y. N 1991 2023;33:4844–58. https://doi.org/10.1093/cercor/bhac384.
[13] Murty VP, Tompary A, Adcock RA, Davachi L. Selectivity in postencoding connectivity with high-level visual cortex is associated with reward-motivated memory. J Neurosci 2017;37:537–45. https://doi.org/10.1523/JNEUROSCI.4032-15.2016.
[14] Beynel L, Powers JP, Appelbaum LG. Effects of repetitive transcranial magnetic stimulation on resting-state connectivity: a systematic review. Neuroimage 2020;211:116596. https://doi.org/10.1016/j.neuroimage.2020.116596.
[15] Fox MD, Buckner RL, Liu H, Chakravarty MM, Lozano AM, Pascual-Leone A. Resting-state networks link invasive and noninvasive brain stimulation across diverse psychiatric and neurological diseases. Proc Natl Acad Sci 2014;111:E4367–75. https://doi.org/10.1073/pnas.1405003111.
[16] Sale M, Mattingley JB, Zalesky A, Cocchi L. Imaging human brain networks to improve the clinical efficacy of non-invasive brain stimulation. Neurosci Biobehav Rev 2015;57:187–98. https://doi.org/10.1016/j.neubiorev.2015.09.010.
[17] Bradley C, Nydam AS, Dux PE, Mattingley JB. State-dependent effects of neural stimulation on brain function and cognition. Nat Rev Neurosci 2022;23:459–75. https://doi.org/10.1038/s41583-022-00598-1.
[18] Sack AT, Paneva J, Küthe T, Dijkstra E, Zwienenberg L, Arns M, Schuhmann T. Target engagement and brain state dependence of transcranial magnetic stimulation: implications for clinical practice. Biol. Psychiatry, Transcranial Magnetic Stimulation 2024;95:536–44. https://doi.org/10.1016/j.biopsych.2023.09.011.
[19] Toth J, Kurtin DL, Brosnan M, Arvaneh M. Opportunities and obstacles in non-invasive brain stimulation. Front Hum Neurosci 2024;18. https://doi.org/10.3389/fnhum.2024.1385427.
[20] Violante IR, Alania K, Cassarà AM, Neufeld E, Acerbo E, Carron R, Williamson A, Kurtin DL, Rhodes E, Hampshire A, Kuster N, Boyden ES, Pascual-Leone A, Grossman N. Non-invasive temporal interference electrical stimulation of the human hippocampus. Nat Neurosci 2023. https://doi.org/10.1038/s41593-023-01456-8.
[21] Inhoff MC, Ranganath C. Dynamic cortico-hippocampal networks underlying memory and cognition: the PMAT framework. In: Hannula DE, Duff MC, editors. The Hippocampus from cells to systems: structure, connectivity, and functional contributions to memory and flexible cognition. Cham: Springer International Publishing; 2017. p. 559–89. https://doi.org/10.1007/978-3-319-50406-3_18.
[22] Ranganath C, Ritchey M. Two cortical systems for memory-guided behaviour. Nat Rev Neurosci 2012;13:713–26. https://doi.org/10.1038/nrn3338.
[23] Ritchey M, Libby LA, Ranganath C. Chapter 3 - cortico-hippocampal systems involved in memory and cognition: the PMAT framework. In: O'Mara S, Tsanov M, editors. Progress in brain Research, the connected Hippocampus. Elsevier; 2015. p. 45–64. https://doi.org/10.1016/bs.pbr.2015.04.001.
[24] Wessel MJ, Beanato E, Popa T, Windel F, Vassiliadis P, Menoud P, Beliaeva V, Violante IR, Abderrahmane H, Dzialecka P, Park C-H, Maceira-Elvira P, Morishita T, Cassara AM, Steiner M, Grossman N, Neufeld E, Hummel FC. Noninvasive theta-burst stimulation of the human striatum enhances striatal activity and motor skill learning. Nat Neurosci 2023;26:2005–16. https://doi.org/10.1038/s41593-023-01457-7.
[25] Wang JX, Rogers LM, Gross EZ, Ryals AJ, Dokucu ME, Brandstatt KL, Hermiller MS, Voss JL. Targeted enhancement of cortical-hippocampal brain networks and associative memory. Science 2014. https://doi.org/10.1126/science.1252900.
[26] Warren KN, Hermiller MS, Nilakantan AS, Voss JL. Stimulating the hippocampal posterior-medial network enhances task-dependent connectivity and memory. Elife 2019;8:e49458.
[27] Brunoni AR, Amadera J, Berbel B, Volz MS, Rizzerio BG, Fregni F. A systematic review on reporting and assessment of adverse effects associated with transcranial direct current stimulation. Int J Neuropsychopharmacol 2011;14:1133–45. https://doi.org/10.1017/S1461145710001690.
[28] Jenkinson M, Beckmann CF, Behrens TEJ, Woolrich MW, Smith SM. Fsl. NeuroImage, 20 YEARS OF fMRI 2012;62:782–90. https://doi.org/10.1016/j.neuroimage.2011.09.015.
[29] Smith SM, Jenkinson M, Woolrich MW, Beckmann CF, Behrens TEJ, Johansen-Berg H, Bannister PR, De Luca M, Drobnjak I, Flitney DE, Niazy RK, Saunders J, Vickers J, Zhang Y, De Stefano N, Brady JM, Matthews PM. Advances in functional and structural MR image analysis and implementation as FSL. NeuroImage, Mathematics in Brain Imaging 2004;23:S208–19. https://doi.org/10.1016/j.neuroimage.2004.07.051.
[30] Jenkinson M, Bannister P, Brady M, Smith S. Improved optimization for the robust and accurate linear registration and motion correction of brain images. Neuroimage 2002;17:825–41. https://doi.org/10.1006/nimg.2002.1132.
[31] Smith RE, Tournier J-D, Calamante F, Connelly A. Anatomically-constrained tractography: improved diffusion MRI streamlines tractography through effective use of anatomical information. Neuroimage 2012;62:1924–38. https://doi.org/10.1016/j.neuroimage.2012.06.005.
[32] Beckmann CF, DeLuca M, Devlin JT, Smith SM. Investigations into resting-state connectivity using independent component analysis. Philos. Trans. R. Soc. B Biol. Sci. 2005;360:1001–13. https://doi.org/10.1098/rstb.2005.1634.
[33] Griffanti L, Salimi-Khorshidi G, Beckmann CF, Auerbach EJ, Douaud G, Sexton CE, Zsoldos E, Ebmeier KP, Filippini N, Mackay CE, Moeller S, Xu J, Yacoub E, Baselli G, Ugurbil K, Miller KL, Smith SM. ICA-based artefact removal and accelerated fMRI acquisition for improved resting state network imaging. Neuroimage 2014;95:232–47. https://doi.org/10.1016/j.neuroimage.2014.03.034.
[34] Salimi-Khorshidi G, Douaud G, Beckmann CF, Glasser MF, Griffanti L, Smith SM. Automatic denoising of functional MRI data: combining independent component analysis and hierarchical fusion of classifiers. Neuroimage 2014;90:449–68. https://doi.org/10.1016/j.neuroimage.2013.11.046.
[35] Schaefer A, Kong R, Gordon EM, Laumann TO, Zuo X-N, Holmes AJ, Eickhoff SB, Yeo BTT. Local-global parcellation of the human cerebral cortex from intrinsic functional connectivity MRI. Cerebr Cortex 2018;28:3095–114. https://doi.org/10.1093/cercor/bhx179.
[36] Yeo BTT, Krienen FM, Sepulcre J, Sabuncu MR, Lashkari D, Hollinshead M, Roffman JL, Smoller JW, Zöllei L, Polimeni JR, Fischl B, Liu H, Buckner RL. The organization of the human cerebral cortex estimated by intrinsic functional connectivity. J Neurophysiol 2011;106:1125–65. https://doi.org/10.1152/jn.00338.2011.
[37] Avants BB, Tustison N, Johnson H. Advanced normalization Tools (ANTS). 2014.
[38] Fischl B. FreeSurfer. NeuroImage, 20 YEARS OF fMRI 2012;62:774–81. https://doi.org/10.1016/j.neuroimage.2012.01.021.
[39] Kurtin DL, Araña-Oiarbide G, Lorenz R, Violante IR, Hampshire A. Planning ahead: predictable switching recruits task-active and resting-state networks. Hum. Brain Mapp. n/a 2023. https://doi.org/10.1002/hbm.26430.
[40] Afshin-Pour B, Soltanian-Zadeh H, Hossein-Zadeh G-A, Grady CL, Strother SC. A mutual information-based metric for evaluation of fMRI data-processing approaches. Hum Brain Mapp 2011;32:699–715. https://doi.org/10.1002/hbm.21057.
[41] Lizier JT, Heinzle J, Horstmann A, Haynes J-D, Prokopenko M. Multivariate information-theoretic measures reveal directed information structure and task relevant changes in fMRI connectivity. J Comput Neurosci 2011;30:85–107. https://doi.org/10.1007/s10827-010-0271-2.
[42] Vergara VM, Miller R, Calhoun V. An information theory framework for dynamic functional domain connectivity. J Neurosci Methods 2017;284:103–11. https://doi.org/10.1016/j.jneumeth.2017.04.009.
[43] Wang Z, Alahmadi A, Zhu D, Li T. Brain functional connectivity analysis using mutual information. In: 2015 IEEE global conference on signal and information processing (GlobalSIP). Presented at the 2015 IEEE global conference on signal and information processing (GlobalSIP); 2015. p. 542–6. https://doi.org/10.1109/GlobalSIP.2015.7418254.
[44] Turkheimer FE, Rosas FE, Dipasquale O, Martins D, Fagerholm ED, Expert P, Váša F, Lord L-D, Leech R. A complex systems perspective on neuroimaging studies of behavior and its disorders. Neuroscientist 2022;28:382–99. https://doi.org/10.1177/1073858421994784.
[45] Power JD, Barnes KA, Snyder AZ, Schlaggar BL, Petersen SE. Spurious but systematic correlations in functional connectivity MRI networks arise from subject motion. Neuroimage 2012;59:2142–54. https://doi.org/10.1016/j.neuroimage.2011.10.018.
[46] Gratton C, Dworetsky A, Coalson RS, Adeyemo B, Laumann TO, Wig GS, Kong TS, Gratton G, Fabiani M, Barch DM, Tranel D, Miranda-Dominguez O, Fair DA, Dosenbach NUF, Snyder AZ, Perlmutter JS, Petersen SE, Campbell MC. Removal of high frequency contamination from motion estimates in single-band fMRI saves data without biasing functional connectivity. Neuroimage 2020;217:116866. https://doi.org/10.1016/j.neuroimage.2020.116866.
[47] Koo TK, Li MY. A guideline of selecting and reporting Intraclass correlation coefficients for reliability Research. J. Chiropr. Med. 2016;15:155–63. https://doi.org/10.1016/j.jcm.2016.02.012.
[48] Rubinov M, Sporns O. Complex network measures of brain connectivity: uses and interpretations. NeuroImage, Computational Models of the Brain 2010;52:1059–69. https://doi.org/10.1016/j.neuroimage.2009.10.003.
[49] Anticevic A, Hu S, Zhang S, Savic A, Billingslea E, Wasylink S, Repovs G, Cole MW, Bednarski S, Krystal JH, Bloch MH, Li C-SR, Pittenger C. Global resting-state functional magnetic resonance imaging analysis identifies frontal cortex, striatal, and cerebellar dysconnectivity in obsessive-compulsive disorder. Biol. Psychiatry, Obsessive-Compulsive Disorder and the Connectome 2014;75:595–605. https://doi.org/10.1016/j.biopsych.2013.10.021.
[50] Preller KH, Burt JB, Ji JL, Schleifer CH, Adkinson BD, Stämpfli P, Seifritz E, Repovs G, Krystal JH, Murray JD, Vollenweider FX, Anticevic A. Changes in global and thalamic brain connectivity in LSD-induced altered states of consciousness are attributable to the 5-HT2A receptor. Elife 2018;7:e35082. https://doi.org/10.7554/eLife.35082.
[51] Prichard D, Theiler J. Generating surrogate data for time series with several simultaneously measured variables. Phys Rev Lett 1994;73:951–4. https://doi.org/10.1103/PhysRevLett.73.951.
[52] Váša F, Mišić B. Null models in network neuroscience. Nat Rev Neurosci 2022;23:493–504. https://doi.org/10.1038/s41583-022-00601-9.
[53] Zalesky A, Fornito A, Bullmore E. On the use of correlation as a measure of network connectivity. Neuroimage 2012;60:2096–106. https://doi.org/10.1016/j.neuroimage.2012.02.001.
[54] Ahmadi H, Fatemizadeh E, Motie-Nasrabadi A. A comparative study of correlation methods in functional connectivity analysis using fMRI data of Alzheimer's patients. J. Biomed. Phys. Eng. 2023;13:125–34. https://doi.org/10.31661/jbpe.v0i0.2007-1134.
[55] Göttlich M, Beyer F, Krämer U. BASCO: a toolbox for task-related functional connectivity. Front Syst Neurosci 2015;9. https://doi.org/10.3389/fnsys.2015.00126.
[56] Westfall PH, Young SS. Resampling-based multiple testing: examples and methods for p-value adjustment. John Wiley & Sons; 1993.

[57] Wang Z, Liu J, Zhong N, Qin Y, Zhou H, Li K. Changes in the brain intrinsic organization in both on-task state and post-task resting state. Neuroimage 2012;62:394–407. https://doi.org/10.1016/j.neuroimage.2012.04.051.
[58] Gonzalez-Castillo J, Handwerker DA, Robinson ME, Hoy CW, Buchanan LC, Saad ZS, Bandettini PA. The spatial structure of resting state connectivity stability on the scale of minutes. Front Neurosci 2014;8. https://doi.org/10.3389/fnins.2014.00138.
[59] Patriat R, Molloy EK, Meier TB, Kirk GR, Nair VA, Meyerand ME, Prabhakaran V, Birn RM. The effect of resting condition on resting-state fMRI reliability and consistency: a comparison between resting with eyes open, closed, and fixated. Neuroimage 2013;78:463–73. https://doi.org/10.1016/j.neuroimage.2013.04.013.
[60] Zhang S, Spoletini LJ, Gold BP, Morgan VL, Rogers BP, Chang C. Interindividual signatures of fMRI temporal fluctuations. Cerebr Cortex 2021;31:4450–63. https://doi.org/10.1093/cercor/bhab099.
[61] Otten LJ, Henson RNA, Rugg MD. State-related and item-related neural correlates of successful memory encoding. Nat Neurosci 2002;5:1339–44. https://doi.org/10.1038/nn967.
[62] Deuker L, Olligs J, Fell J, Kranz TA, Mormann F, Montag C, Reuter M, Elger CE, Axmacher N. Memory consolidation by replay of stimulus-specific neural activity. J Neurosci 2013;33:19373–83. https://doi.org/10.1523/JNEUROSCI.0414-13.2013.
[63] Dewar M, Alber J, Cowan N, Sala SD. Boosting long-term memory via wakeful rest: intentional rehearsal is not necessary, consolidation is sufficient. PLoS One 2014;9:e109542. https://doi.org/10.1371/journal.pone.0109542.